

Communication

Functional Segmentation Method for the Design of Compact Adiabatic Devices

Tu-Lu Liang^{1,2,3,*} , Xi Cheng^{4,*}, Mei Yu^{1,2,3} , Jin Shi^{1,2,3}, Gangxiong Wu^{1,2,3}, Ruirui Jiang^{1,2,3}, Weiwei Rong^{2,5} and Wei Shao⁶

¹ School of Information Science and Technology, Nantong University, Nantong 226019, China; yumei@ntu.edu.cn (M.Y.); jinshi@ntu.edu.cn (J.S.); wxg@ntu.edu.cn (G.W.); jrr@ntu.edu.cn (R.J.)

² Research Center for Intelligent Information Technology, Nantong University, Nantong 226019, China; rongweiwei@ntu.edu.cn

³ Nantong Key Laboratory of Advanced Microwave Technology, Nantong University, Nantong 226019, China

⁴ School of Computer and Information Engineering, Xinjiang Agricultural University, 311 Nongda Dong Lu, Urumqi 830052, China

⁵ School of Pharmacy, Nantong University, Nantong 226019, China

⁶ School of Physics, University of Electronic Science and Technology of China, Chengdu 610054, China; weishao@uestc.edu.cn

* Correspondence: liangtulu@ntu.edu.cn (T.-L.L.); chengxi@xjau.edu.cn (X.C.)

Abstract: In this study, a functional segmentation method for the design of adiabatic devices is presented. This method can be applied to calculate the compact adiabatic waveguide shapes for adiabatic taper waveguides and adiabatic mode converters. We introduce two algorithms, namely the quadratic function segmentation design for the adiabatic taper waveguide and the cubic function segmentation design for the adiabatic mode coupler. The design shows that for each segment, there is no need for separate simulations to obtain the length of each segment, and only the length of each segment can be determined by equations. This approach is much less cumbersome than other numerical design methods for adiabatic devices. The proposed functional segmentation design requires only a device length of 36 μm to achieve 95% power transfer efficiency, while a traditional linear-shape connection requires a device length of 54 μm to achieve the same power transfer efficiency. Therefore, the device designed by the function segmentation method has better compactness compared to the conventional linear-shape connection design of adiabatic devices.



Citation: Liang, T.-L.; Cheng, X.; Yu, M.; Shi, J.; Wu, G.; Jiang, R.; Rong, W.; Shao, W. Functional Segmentation Method for the Design of Compact Adiabatic Devices. *Photonics* **2023**, *10*, 1019. <https://doi.org/10.3390/photonics10091019>

Received: 17 July 2023

Revised: 23 August 2023

Accepted: 3 September 2023

Published: 6 September 2023



Copyright: © 2023 by the authors. Licensee MDPI, Basel, Switzerland. This article is an open access article distributed under the terms and conditions of the Creative Commons Attribution (CC BY) license (<https://creativecommons.org/licenses/by/4.0/>).

Keywords: adiabatic devices; adiabatic mode evolution; integrated optics; optical waveguide design

1. Introduction

In photonic integrated circuits, energy is transferred in different structures, and even when it is transferred in the same structure, the structural parameters will change, making it necessary to design a connection structure to transfer energy from one module to another [1–5]. In order to realize the design of connection structures, adiabatic devices based on the adiabatic mode evolution play an increasingly important role [6–8]. In adiabatic devices, the designated mode at the input slowly evolves into the designated mode at the output. The output mode can be the same or different from the input mode, which is referred to as transfer efficiency when the modes are the same and conversion efficiency when the modes are different. No other unwanted modes were significantly excited during this evolution. The power transfer/conversion efficiency from the designated input mode to the designated output mode is very high.

One way to achieve adiabatic mode evolution transfer is to connect different functional units linearly. However, the resulting device structure has a long size [9], which runs counter to the direction of optical integration towards higher integration. The analytical method can reduce the size of the adiabatic device. However, the analytical method design for adiabatic devices is only suitable for simple device structures, and the analytical method is not universal [6–14]. The methods proposed in refs. [6–8] are only suitable for the design

of adiabatic couplers and are not suitable for the design of adiabatic tapered waveguides or adiabatic mode couplers in this study. Refs. [10–14] are all analytical designs of adiabatic tapered waveguides, in which ref. [10] describes mode propagation using a ray model, thus perfecting the analytical design rules for tapered waveguides proposed by Milton and Burns. In ref. [14], an equivalent waveguide concept was proposed. This concept converts a straight waveguide into an equivalent conformal structure via conformal mapping and is applied to the design and analysis of a fully adiabatic tapered waveguide. These analytical methods are only suitable for the design of specific types of adiabatic devices. They are not suitable for the design of other types of adiabatic devices, which greatly limits the wide range of applications of these analytical methods. In the last three years, in order to design adiabatic devices with complicated three-dimensional (3D) geometries, numerical design methods [15–17] have been proposed. Numerical methods can handle various types of adiabatic devices and can also be used to design device structures with geometric shapes, which is convenient for applications. The numerical design methods for the adiabatic device [15–17] are calculated accurately. The methods are universal, but they require simulations for each section. Determining how many sections are divided, how many simulations are required, and selecting device length from simulation results increase the complexity of the design of the adiabatic device.

Therefore, in order to eliminate the need for simulations for each section, this study proposes a functional segmentation design method for the design of adiabatic taper waveguides and adiabatic mode converters. For the design of adiabatic taper waveguides, the device size of the quadratic function design is much smaller than that of the conventional linear-shape connection design (see Section 2). For the design of adiabatic mode converters, the cubic function segmentation design method in this study is better than the analytical method in ref. [9] (see Section 3).

2. Quadratic Functional Segmentation Design of Adiabatic Taper Waveguides

Figure 1 shows two strip waveguides with different waveguide widths. The silicon core in the strip waveguide in Figure 1a has a narrow waveguide width W_I , and the silicon core in the strip waveguide in Figure 1b has a wide waveguide width W_F . The purpose is to design an adiabatic taper waveguide structure that connects the narrow and wide strip waveguides in Figure 1 and efficiently transfers energy from one strip waveguide to the other with the shortest possible device length. The wavelength of the light beam is set to $1.55 \mu\text{m}$.

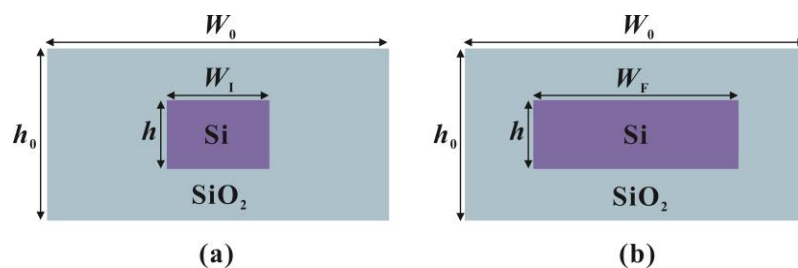


Figure 1. (a) Narrow strip waveguides; (b) wide strip waveguides.

A quadratic function is used to shorten the device length of the adiabatic taper waveguide. As shown in Figure 2, assuming the x -axis is horizontal and the y -axis is vertical, the expression for the quadratic function is:

$$y = Ax^{1/2} \tag{1}$$

where A is a constant.

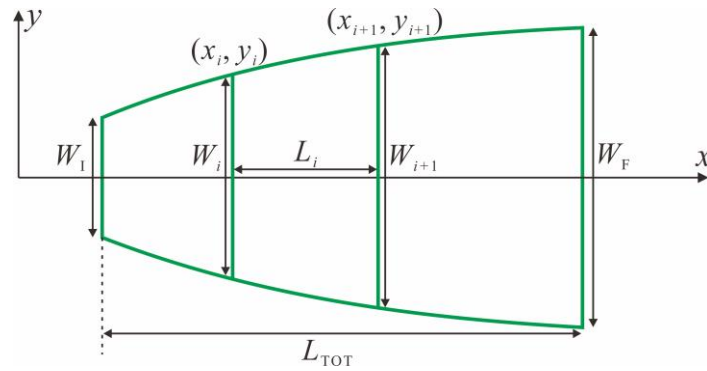


Figure 2. Schematic diagram of the quadratic function design.

As shown in Figure 2, the width is denoted by $W_I = y_I$ at the left end and $W_F = y_F$ at the right end. The absolute length is $L_{TOT} = x_F - x_I$. Similar to the numerical design methods for adiabatic devices that require segmentation, the functional segmentation design presented here also requires the entire structure to be divided into several distinct sections. A section is randomly intercepted in the quadratic function, and the coordinates of the initial and ending ends of the section in the upper part function are (x_i, y_i) and (x_{i+1}, y_{i+1}) , respectively. Substituting the coordinates (x_i, y_i) and (x_{i+1}, y_{i+1}) into Equation (1) yields:

$$y_i = Ax_i^{1/2} \tag{2}$$

$$y_{i+1} = Ax_{i+1}^{1/2} \tag{3}$$

Since the width $W_i = 2y_i$ and the width $W_{i+1} = 2y_{i+1}$, substituting into Equations (2) and (3), respectively, yields:

$$W_i = 2Ax_i^{1/2} \tag{4}$$

$$W_{i+1} = 2Ax_{i+1}^{1/2} \tag{5}$$

Squaring both sides of Equations (4) and (5) yields:

$$W_i^2 = 4A^2x_i \tag{6}$$

$$W_{i+1}^2 = 4A^2x_{i+1} \tag{7}$$

Subtract Equation (6) from Equation (7) to obtain:

$$L_i = \frac{W_{i+1}^2 - W_i^2}{4A^2} \tag{8}$$

Considering $W_i = W_I$ and $W_{i+1} = W_F$, we can obtain the expression for the coefficient A:

$$A = \frac{1}{2} \sqrt{\frac{W_F^2 - W_I^2}{L_{TOT}}} \tag{9}$$

Substituting the expression (9) of the coefficient A into the Equation (8) gives the length of each section:

$$L_i = \frac{L_{TOT}}{W_F^2 - W_I^2} (W_{i+1}^2 - W_i^2) \tag{10}$$

Equation (10) is used to calculate the length for each section in adiabatic taper waveguides. This equation is free from axial limitations and only depends on the structural parameters to be designed. For each section, the input and output widths W_i and W_{i+1} are connected linearly.

As shown in Figure 1, the width of SiO₂ is $W_0 = 10 \mu\text{m}$, the thickness of SiO₂ is $h_0 = 1.5 \mu\text{m}$, the thickness of silicon is $h = 300 \text{ nm}$, and the width of silicon increases from $W_1 = 2 \mu\text{m}$ to $W_F = 8 \mu\text{m}$. The uniform segmentation is used to divide the width from $W_1 = 2 \mu\text{m}$ to $W_F = 8 \mu\text{m}$ intervals ($\Delta W = 0.1 \mu\text{m}$) into $N = 60$ sections. The higher the number of segments, the closer the shape is to the shape of the true quadratic function, but this also leads to higher computational demands. The widths of the input and output of the i -th section are $W_i = [2 + (i - 1) \times 0.1] \mu\text{m}$ and $W_{i+1} = (2 + i \times 0.1) \mu\text{m}$, respectively, where i increases from 1 to N . According to Equation (10), the length for each section can be obtained.

Each section is constructed according to the input width W_i and output width W_{i+1} of each section. The length of each section is obtained by Equation (10), and then all the sections are spliced to form a complete waveguide shape. Then, the power transfer efficiency curve of the entire structure can be obtained by the Finite-difference time-domain (FDTD) method or the Eigenmode Expansion (EME) method, as shown in Figure 3. The figure shows the lengths corresponding to the power transfer efficiency, which can be used in practical applications.

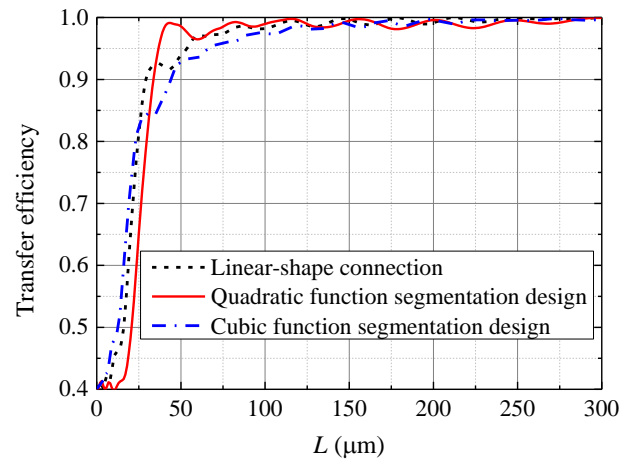


Figure 3. Power transfer efficiency of the designed adiabatic taper waveguide; the power transfer efficiencies are plotted for the conventional linear shape connection and the cubic functional segmentation for comparison.

As shown in Figure 3, when 95% power transfer efficiency is required, the length required for the quadratic function segmentation design is $36 \mu\text{m}$, while the length required for the linear-shape connection is $54 \mu\text{m}$. When 99% power transfer efficiency is required, the function segmentation design requires a length of $78 \mu\text{m}$, while the linear-shape connection requires a length of $109 \mu\text{m}$. As a result, the quadratic function segmentation design is designed with a much smaller device size than the conventional linear-shape connection.

Ref. [15] defines the adiabatic regime. When the power loss is greater than 10%, the adiabatic performance is poor. We can say that we are in an acceptable adiabatic regime when the power loss is less than or equal to 10%. Therefore, we choose a minimum power transfer efficiency of 90%. We can also choose a power transfer efficiency of 95% when we need a better adiabatic regime. Certainly, if someone wishes to pursue a better adiabatic regime, they can also choose a higher power transfer efficiency, such as 99% or even higher.

3. Cubic Functional Segmentation Design of Adiabatic Mode Converters

Figure 4 shows that the strip waveguide has a lower cladding of SiO₂ and an upper cladding of Si₃N₄, which makes the strip vertically asymmetric and allows mode conversion between different modes. The goal is to design an adiabatic mode converter that efficiently converts one mode at the input to another mode at the output with the shortest possible device length. The wavelength of the light beam is set to $1.55 \mu\text{m}$.

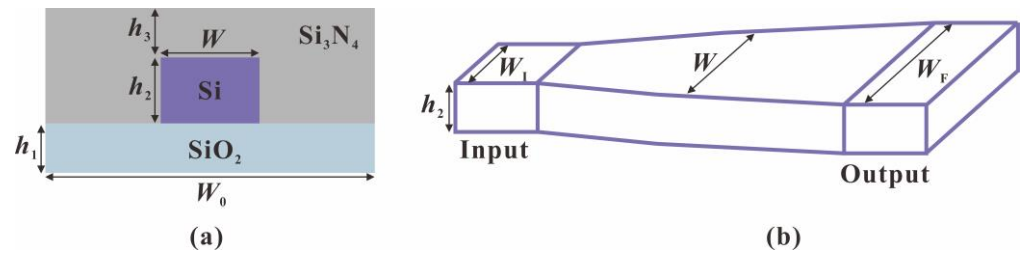


Figure 4. (a) Cross-section of the strip waveguide; (b) top view of the strip waveguide.

As shown in Figure 5, considering the horizontal direction as the x -axis and the vertical direction as the y -axis, the expression for the cubic function is:

$$y = A(x - B)^3 \tag{11}$$

where A and B are constants.

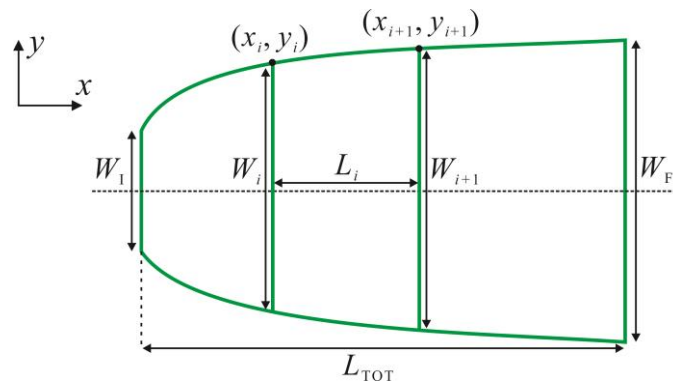


Figure 5. Schematic diagram of the cubic function design.

Input width $W_1 = 2y_1$, output width $W_F = 2y_F$, and absolute length $L_{TOT} = x_F - x_1$; substitute coordinates (x_i, y_i) and (x_{i+1}, y_{i+1}) into Equation (11) to obtain:

$$y_i = A(x_i - B)^3 \tag{12}$$

$$y_{i+1} = A(x_{i+1} - B)^3 \tag{13}$$

where $y_{i+1} > y_i > 0$, x_i and x_{i+1} are calculated from Equation (11).

Since the input width is $W_i = 2y_i$ and the output width is $W_{i+1} = 2y_{i+1}$, substituting Equations (12) and (13) yields the following:

$$\frac{W_i}{2} = A(x_i - B)^3 \tag{14}$$

$$\frac{W_{i+1}}{2} = A(x_{i+1} - B)^3 \tag{15}$$

Equations (14) and (15) are opened on both sides of the equation to yield:

$$x_i = \sqrt[3]{\frac{W_i/2}{A}} + B \tag{16}$$

$$x_{i+1} = \sqrt[3]{\frac{W_{i+1}/2}{A}} + B \tag{17}$$

Subtract Equation (16) from Equation (17) to obtain:

$$L_i = A \left(\sqrt[3]{\frac{W_{i+1}}{2}} - \sqrt[3]{\frac{W_i}{2}} \right) \tag{18}$$

Considering $W_i = W_I$ and $W_{i+1} = W_F$, give the expression for the coefficient A:

$$A = \frac{L_{TOT}}{\sqrt[3]{W_F/2} - \sqrt[3]{W_I/2}} \tag{19}$$

Substituting the expression (19) of the coefficient A into Equation (18) yields the individual fragments:

$$L_i = \frac{L_{TOT}}{\sqrt[3]{\frac{W_F}{2}} - \sqrt[3]{\frac{W_I}{2}}} \left(\sqrt[3]{\frac{W_{i+1}}{2}} - \sqrt[3]{\frac{W_i}{2}} \right) \tag{20}$$

Equation (20) is used to calculate the length for each section, which is independent of the coordinates and is only related to the structural parameters to be designed.

As shown in Figure 6, strip waveguides of different widths W are simulated using a time-domain simulation algorithm to obtain the effective refractive index for each mode corresponding to each width. The thickness of the silicon core is $h_2 = 220$ nm. From the figure, it can be determined that the width $W_0 = 0.75 \mu\text{m}$ of the mode hybrid region appears. To achieve mode conversion, the input width W_I and output width W_O of the waveguide need to meet the following conditions: $W_I < W_0 < W_F$. After some simulation, the Eigenmode Expansion (EME) simulator from Lumerical is used to determine whether mode conversion really exists. Finally, it is determined that the input waveguide width is $W_I = 0.69 \mu\text{m}$ and the output waveguide width is $W_F = 0.83 \mu\text{m}$.

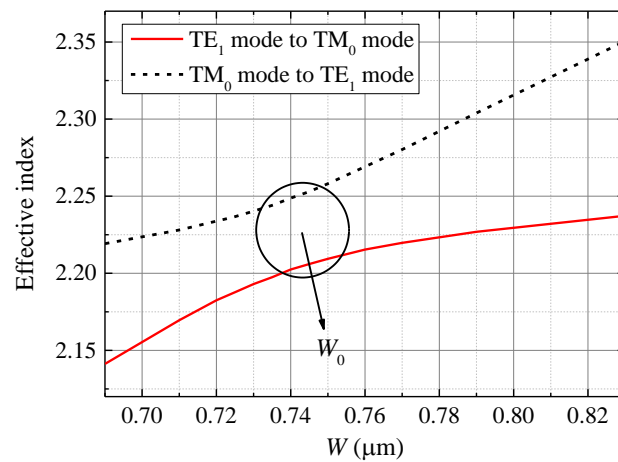


Figure 6. Effective refractive index at different widths of adiabatic mode converters.

This example uses non-uniform segmentation to divide the width from $W = 0.69 \mu\text{m}$ to $W = 0.73 \mu\text{m}$ at intervals $\Delta W_{Ni} = 0.002 \mu\text{m}$ into 20 sections; divide the width from $W = 0.73 \mu\text{m}$ to $W = 0.78 \mu\text{m}$ at intervals $\Delta W_{Hi} = 0.001 \mu\text{m}$ into 50 sections; divide the width from $W = 0.78 \mu\text{m}$ to $W = 0.83 \mu\text{m}$ at intervals $\Delta W_{Ni} = 0.002 \mu\text{m}$ into 25 sections. This section satisfies that the interval ΔW_{Hi} of the hybrid region is less than twice the interval ΔW_{Ni} of the non-mode hybrid region, that is, $\Delta W_{Hi} < 2\Delta W_{Ni}$.

Each section is constructed according to the input width W_i and output width W_{i+1} of each section. The length of each section is obtained by Equation (20), and then all the sections are spliced to form a complete waveguide shape. Then, the power conversion efficiency curve of the entire structure can be obtained by the Finite-difference time-domain

(FDTD) method or the Eigenmode Expansion (EME) method, as shown in Figure 7. The figure shows the lengths corresponding to the power conversion efficiency, which can be used in practical applications.

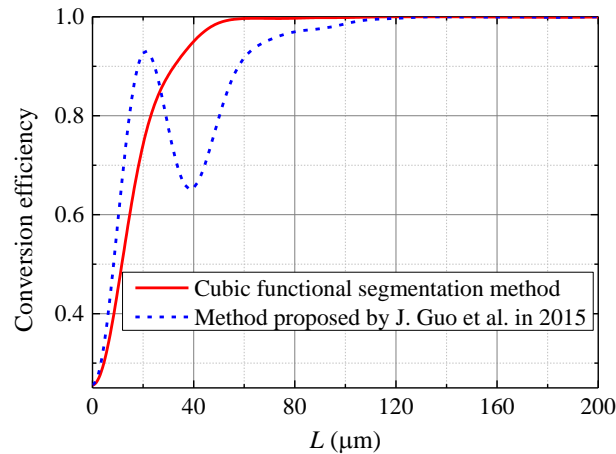


Figure 7. Power conversion efficiency of the designed adiabatic mode converter; the power conversion efficiency is also plotted for the method proposed by J. Guo et al. in Ref. [9] for comparison.

As shown in Figure 7, when 90% power conversion efficiency is required, the length required for the cubic functional segmentation design is 37 μm . When 99% power transfer efficiency is required, the cubic functional segmentation design requires a length of 59 μm . In Figure 7, the analytical method design in ref. [9] is added as a comparison, which can better reflect the advantages of the cubic functional segmentation technique in this study. It can be seen from the figure that the method in ref. [9] has obvious oscillation, indicating a large energy loss. Therefore, the effect of the cubic functional segmentation design is better than that of the design in ref. [9]. The choice of total length in practical applications requires balancing the power conversion efficiency with the length requirement. Small device lengths can be chosen to achieve higher integration design goals when the conversion efficiency is not too high.

The variation in the effective refractive index with the width of the waveguide is one way in which we can determine the existence of a mode hybridization region. In this way, it is determined that there is mode conversion in some areas; for example, it is determined that there is mode conversion near $W_0 = 0.75 \mu\text{m}$ in Figure 6. To achieve mode conversion, the input width W_I and output width W_O of the waveguide need to meet the following conditions: $W_I < W_0 < W_F$. After some simulation, the Eigenmode Expansion (EME) simulator from Lumerical is used to determine whether mode conversion really exists. Finally, it is determined that when the input waveguide width is $W_I = 0.69 \mu\text{m}$, and the output waveguide width is $W_F = 0.83 \mu\text{m}$, the mode conversion can indeed be realized. The conversion efficiency is shown in Figure 7. It is proven that there is indeed a mode conversion from width $W_I = 0.69 \mu\text{m}$ to width $W_F = 0.83 \mu\text{m}$.

Through various works [1,2], it has been shown that quadratic function shapes generally give more efficient adiabatic taper waveguides compared to linear-shape designs. Ref. [9] shows that cubic function shapes often give efficient adiabatic mode converters. Therefore, a quadratic function segmentation method is developed for the design of adiabatic taper waveguides and a cubic function segmentation method for the design of adiabatic mode converters. Certainly, the cubic function segmentation method can also be used in the design of adiabatic taper waveguides, but the results are poor, as shown in Figure 3. It can be seen from Figure 3 that the transfer efficiency of the adiabatic taper waveguide designed with cubic function segmentation is much worse than that of the adiabatic taper waveguide designed with quadratic function segmentation and even worse than that of the linear-shape connection.

4. Conclusions

In this work, we propose a functional segmentation design method for adiabatic devices. The proposed method can be used to help calculate the compact waveguide shapes for adiabatic devices. Two algorithms are mainly introduced, namely the quadratic function segmentation design for the adiabatic taper waveguide and the cubic function segmentation design for the adiabatic mode converter. From the design results, it can be seen that the device structure designed by the proposed functional segmentation design method has good compactness. In contrast to other numerical design methods for adiabatic devices, the device length for each section can be determined by using only the equation. Additionally, there is no need to simulate each section to obtain the corresponding device length, which is much less cumbersome.

Author Contributions: Conceptualization, T.-L.L.; formal analysis, T.-L.L. and M.Y.; investigation, G.W. and J.S.; methodology, T.-L.L. and R.J.; project administration, X.C.; writing—original draft preparation, T.-L.L. and X.C.; writing—review and editing, T.-L.L., W.R. and W.S. All authors have read and agreed to the published version of the manuscript.

Funding: This work was partially supported by the National Natural Science Foundation of China (62161048, 62104117, and 62201292), partially supported by the Nantong Science and Technology Plan Project (JC12022087), and partially supported by the Natural Science Research Project of Jiangsu Higher Education Institutions (22KJB140004, 23KJB510024).

Institutional Review Board Statement: Not applicable.

Informed Consent Statement: Not applicable.

Data Availability Statement: Not applicable.

Conflicts of Interest: The authors declare no conflict of interest.

References

1. Burns, W.K.; Milton, A.F.; Lee, A.B. Optical waveguide parabolic coupling horns. *Appl. Phys. Lett.* **1977**, *30*, 28–30. [[CrossRef](#)]
2. Milton, A.F.; Burns, W.K. Mode coupling in optical waveguide horns. *IEEE J. Quantum Electron.* **1977**, *13*, 828–835. [[CrossRef](#)]
3. Dai, D.; He, S.; Tsang, H.K. Bilevel mode converter between a silicon nanowire waveguide and a larger waveguide. *J. Lightwave Technol.* **2006**, *24*, 2428–2433.
4. Dai, D.; Bowers, J.E. Novel concept for ultracompact polarization splitter-rotator based on silicon nanowires. *Opt. Express* **2011**, *19*, 10940–10949. [[CrossRef](#)] [[PubMed](#)]
5. Dai, D.; Tang, Y.; Bowers, J.E. Mode conversion in tapered submicron silicon ridge optical waveguides. *Opt. Express* **2012**, *20*, 13425–13439. [[PubMed](#)]
6. Sun, X.; Liu, H.C.; Yariv, A. Adiabaticity criterion and the shortest adiabatic mode transformer in a coupled-waveguide system. *Opt. Lett.* **2009**, *34*, 280–282. [[PubMed](#)]
7. Ng, V.; Tuniz, A.; Dawes, J.M.; de Sterke, C.M. Insights from a systematic study of crosstalk in adiabatic couplers. *OSA Continuum* **2019**, *2*, 629–639. [[CrossRef](#)]
8. Ramadan, T.A.; Scarmozzino, R.; Osgood, R.M. Adiabatic couplers: Design rules and optimization. *J. Light. Technol.* **1998**, *16*, 277–283. [[CrossRef](#)]
9. Guo, J.; Zhao, Y. Analysis of mode hybridization in tapered waveguides. *IEEE Photon. Tech. Lett.* **2015**, *27*, 2441–2444. [[CrossRef](#)]
10. Fu, Y.; Ye, T.; Tang, W.; Chu, T. Efficient adiabatic silicon-on-insulator waveguide taper. *Photon. Res.* **2014**, *2*, A41–A44. [[CrossRef](#)]
11. Marcatili, E. Dielectric tapers with curved axes and no loss. *IEEE J. Quantum Electron.* **1985**, *21*, 307–314. [[CrossRef](#)]
12. Weder, R. Dielectric three-dimensional electromagnetic tapers with no loss. *IEEE J. Quantum Electron.* **1988**, *24*, 775–779. [[CrossRef](#)]
13. Sakai, J.; Marcatili, E.A.J. Lossless dielectric tapers with 3-dimensional geometry. *J. Light. Technol.* **1991**, *9*, 386–393. [[CrossRef](#)]
14. Lee, C.T.; Wu, M.L.; Sheu, L.G.; Fan, P.L.; Hsu, J.M. Design and analysis of completely adiabatic tapered waveguides by conformal mapping. *J. Light. Technol.* **1997**, *15*, 403–410.
15. Liang, T.L.; Tu, Y.; Chen, X.; Huang, Y.; Bai, Q.; Zhao, Y.; Zhang, J.; Yuan, Y.; Li, J.; Yi, F.; et al. A Fully Numerical Method for Designing Efficient Adiabatic Mode Evolution Structures (Adiabatic Taper, Coupler, Splitter, Mode Converter) Applicable to Complex Geometries. *J. Light. Technol.* **2021**, *39*, 5531–5547. [[CrossRef](#)]

16. Liang, T.L.; Cheng, X.; Yu, M.; Zhang, L.; Shi, J.; Shao, W. Numerical method for designing ultrashort and efficient adiabatic mode converters. *J. Opt. Soc. Am. B* **2022**, *39*, 2637–2642. [[CrossRef](#)]
17. Liang, T.L.; Cheng, X.; Yu, M.; Zhang, L.; Shi, J.; Wu, G.; Rong, W.; Shao, W. Numerical Method for the Design of Compact Adiabatic Devices with Multiple Parameter Variations. *Photonics* **2023**, *10*, 517. [[CrossRef](#)]

Disclaimer/Publisher’s Note: The statements, opinions and data contained in all publications are solely those of the individual author(s) and contributor(s) and not of MDPI and/or the editor(s). MDPI and/or the editor(s) disclaim responsibility for any injury to people or property resulting from any ideas, methods, instructions or products referred to in the content.